Available online at www.sciencedirect.com
ScienceDirect
Trans. Nonferrous Met. Soc. China 33(2023) 2523−2534
Transactions of Nonferrous Metals Society of China
www.tnmsc.cn

Synthesis of mullite by high temperature reaction to realize nontoxic and efficient recycling of vanadium slag chlorination residue

Shi-yuan LIU[1], Wei-hua XUE[1], Li-jun WANG[1], Kuo-chih CHOU[2]

1. Collaborative Innovation Center of Steel Technology, University of Science and Technology Beijing, Beijing 100083, China;
2. State Key Laboratory of Advanced Metallurgy, University of Science and Technology Beijing, Beijing 100083, China

Received 22 February 2022; accepted 12 May 2022

Abstract: The compositions of the leaching residue obtained by chlorination method to extract valuable elements (Ti, Cr, Fe, Mn and V) from vanadium slag were mainly Al_2O_3 and SiO_2 with a small amount of hazardous elements Cr and V. In order to reduce the pollution of V and Cr to the environment, a novel method for nontoxic and efficient recycling of leaching residue was proposed. Mullite with high compressive strength of 133.345 MPa and bulk density of 3.20 g/cm^3 was successfully synthesized by using leaching residue as raw material, adding appropriate SiO_2 and roasting at 1600 ℃ for 5 h. The trace element Ti and hazardous elements V and Cr in leaching residue entered the mullite lattice in the high temperature reaction process to form a solid solution, which were stabilized in the mullite phase. The synthesized samples were tested by toxicity characteristic leaching procedure (TCLP) and GB5085.3—2007. The results showed that mullite met the toxic leaching standard and was a nontoxic product.

Key words: leaching residue; vanadium slag; comprehensive utilization; highly toxic hexavalent chromium; mullite; toxicity characteristic leaching procedure

1 Introduction

Vanadium slag containing valuable elements Fe, V, Cr, Ti, Mn and Si is an important resource. The content of SiO_2 in vanadium slag can reach 20.88 wt.% [1]. The extraction of Cr and V from vanadium slag is realized by the traditional salt (Na_2CO_3, NaOH and CaO) roasting method [2,3] and acid leaching process [4,5]. However, about 1.2×10^6 t of tailing containing a large amount of valuable elements (Si, Fe, Mn and Ti) and a small amount of hazardous elements (V and Cr) is yearly abandoned as solid waste [6], which waste resources and pollute environment. LIU et al [7] reported sodium removal of residue-blast furnace ironmaking and high-value utilization including vanadium−titanium black porcelain and solar collector plate. The blast furnace smelting process could use the iron in the residue, and Si entered the slag. This process had high temperature, high energy consumption and low element utilization. Ti and Fe in residue were extracted by ammonium sulfate leaching and were used to synthesize $LiFePO_4$ [8]. ZHANG et al [9] proposed that Fe, Cr, V and Ti in residue were recycled by reduction−separation−leaching−solvent extraction. LI et al [10] pointed out that Fe in residue was extracted by sulfuric acid roasting and Al and Si were used to synthesize petroleum proppants, such as (α-$Al_2O_3\cdot3Al_2O_3\cdot2SiO_2$). In order to effectively utilize vanadium slag, LIU et al [11] extracted Fe, Mn, Ti, Cr and V from vanadium slag by chlorination of vanadium slag in molten salt system

Corresponding author: Li-jun WANG, Tel: +86-15210906865, E-mail: lijunwang@ustb.edu.cn
DOI: 10.1016/S1003-6326(23)66278-8

with $AlCl_3$ as chlorination agent. In the previous work, the efficient extraction of valuable elements (Cr, V, Mn, Ti and Fe) was achieved. Meanwhile, Fe−Mn alloy, V−Cr alloy and TiO_2, were obtained by high-value utilization of valuable elements (Fe, V, Ti, Mn and Cr). However, the residue has not been effectively used. The compositions of leaching residue are mainly Al_2O_3 and SiO_2 with a small amount of hazardous elements Cr and V.

Al_2O_3 and SiO_2 are the main components of mullite [12]. As a ceramic material, mullite has the following excellent properties: good chemical and thermal stability, low thermal expansion, good catalytic adsorption performance, good compressive strength and high temperature creep resistance, etc [12−18]. Due to the above advantages, mullite is considered as an advanced material with development prospects in the application fields of refractories and structural ceramics [18]. The chemical expression of mullite is $Al_2(Al_{2+2x}Si_{2-2x})O_{10-x}$ (x is the atomic number of Al^{3+} replacing Si^{4+}; $0.18 < x < 0.88$). It has a highly open space structure and can accommodate metals such as Ti, V, Cr, Mn and Fe into its lattice to form solid solutions, which makes mullite form different crystal structures and micro-morphology characteristics according to its chemical composition and preparation methods, such as needle-like, whisker-like and columnar structure [19−21]. Various methods have been used to prepare highly reactive mullite powders, which mainly include solid−state reaction, hydro- thermal treatment, chemical vapor deposition, alcohol−salt solution, precipitation and sol−gel methods [13,16,19,22].

Natural mullite minerals are rare, and the preparation of commercial mullite using industrial Al_2O_3 and SiO_2 as raw materials has high cost and is difficult to obtain good economic benefits. A large amount of silicon-containing vanadium slag is produced every year. The current process cannot effectively utilize the silicon in the vanadium slag. As the raw material of mullite, the silicon in the vanadium slag can greatly reduce the cost of mullite and realize the effective utilization of the silicon in the vanadium slag. Since there are parts of hazardous vanadium and chromium in silicon-containing slag, it will pollute the environment when it is not treated.

In this work, a novel method to stabilize the harmful elements V and Cr in chlorinated tailings produced from vanadium slag with mullite phase was proposed. The influences of temperature, time and the mass ratio of Al_2O_3 to SiO_2 were investigated to synthesize pure mullite. This process realized comprehensive utilization of vanadium slag and at the same time solidified the hazardous elements V and Cr in the residue into the mullite phase, which realized the harmless and high-value utilization of the residue.

2 Experimental

The vanadium slag used in the experiment was from Panzhihua, Sichuan Province, China. After the vanadium slag was crushed and sieved, the particle size was between 49 and 74 μm. All the experimental materials such as NaCl, KCl, $AlCl_3$, Al_2O_3 and SiO_2 are reagent-grade powders.

2.1 Pretreatment of vanadium slag

The mixture of 36.14 g $AlCl_3$, 24.1 g vanadium slag, 26.66 g NaCl and 33.33 g KCl was heated at 900 °C for 8 h. During the experiment, argon was used as the protective gas, and the flow rate was 400 mL/min. The product was washed with deionized water after molten salt electrolysis to remove chloride from the sample. After filtration, the residue was dried at 105 °C for 12 h. The composition of the residue is shown in Table 1. The phase of the residue is shown in Fig. 1, which shows that the main components of the leaching residue are Al_2O_3 and SiO_2, and the main phases of the leaching residue are mullite, Al_2O_3 and SiO_2.

Table 1 Composition of leaching residue (wt.%)

Al_2O_3	SiO_2	Cl	TiO_2	V_2O_3	Cr_2O_3	MnO	Fe_2O_3
69.90	24.20	0.54	2.75	1.56	0.12	0.017	0.16

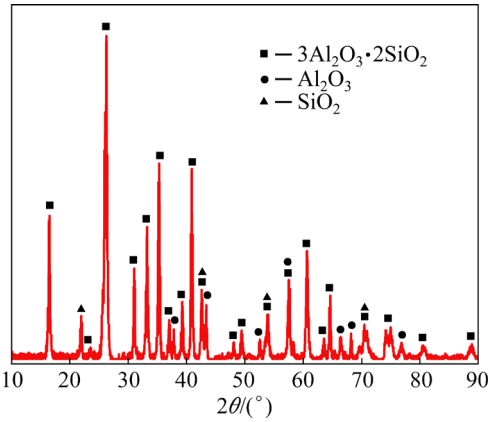

Fig. 1 XRD pattern of leaching residue

2.2 Synthesis of mullite by high temperature roasting

The leaching residue was mixed with different proportions of SiO_2 and put into the ball mill for 12 h to make them mixed. The mass ratio of Al_2O_3 to SiO_2 reached 2.80, 2.55 and 2.10, respectively. The material was pressed into a cylinder with a height of 2 cm and a diameter of 2 cm under the pressure of 20 MPa. The sample was put into the furnace at room temperature and roasted at 1400, 1500 and 1600 °C for 3, 5 and 7 h, respectively.

2.3 Characterization and toxicity test of mullite

The phases of products were detected by X-ray diffraction (XRD; TTR III, Rigaku Corporation, Japan) in 2θ range of 10°−90° to analyze the phase composition. The samples were observed by scanning electron microscopy (SEM with EDS) (Zeiss Ultra 55) to analyze the microstructure and the distribution of elements in the products. Morphology and diffraction of samples were analyzed by TEM (Tecnai G2 F30 S-TWIN). The valence of elements of products was analyzed by XPS (Thermo Scientific K-Alpha$^+$).

Compressive strength and other mechanical properties of the samples were tested by tensile compression equipment. The density of the product was analyzed by gas volume density tester.

The content of migrating hazardous substances in the product was tested by the toxicity characteristic leaching procedure (TCLP) standard and GB5085.3—2007 standard. The content of each element in the leaching solution was determined by inductively coupled plasma optical emission spectroscopy (ICP-AES, SPECTRO ARCOS EOP, SPECTRO Analytical Instruments GmbH).

3 Results and discussion

3.1 Synthesis of mullite from leaching residue

3.1.1 Thermodynamic analysis of synthetic mullite

Figure 2(a) shows the partial phase diagram of Al_2O_3 and SiO_2 binary system calculated by FactSage 8.1. The composition and temperature have a great influence on the phase composition of binary system. According to the difference of phases, there are five regions in the Fig. 2(a) when the mass ratio of Al_2O_3 to SiO_2 increases from 2 to 3 and temperature increases from 1400 to 1650 °C. Only mullite phase is obtained in one of the areas. Thus, in order to prepare pure mullite, the temperature and mass ratio of Al_2O_3 to SiO_2 should be strictly controlled. The original mass ratio of Al_2O_3 to SiO_2 in the leaching residue is 2.8 and pure mullite phase will be obtained in the temperature range from 1400 to 1650 °C.

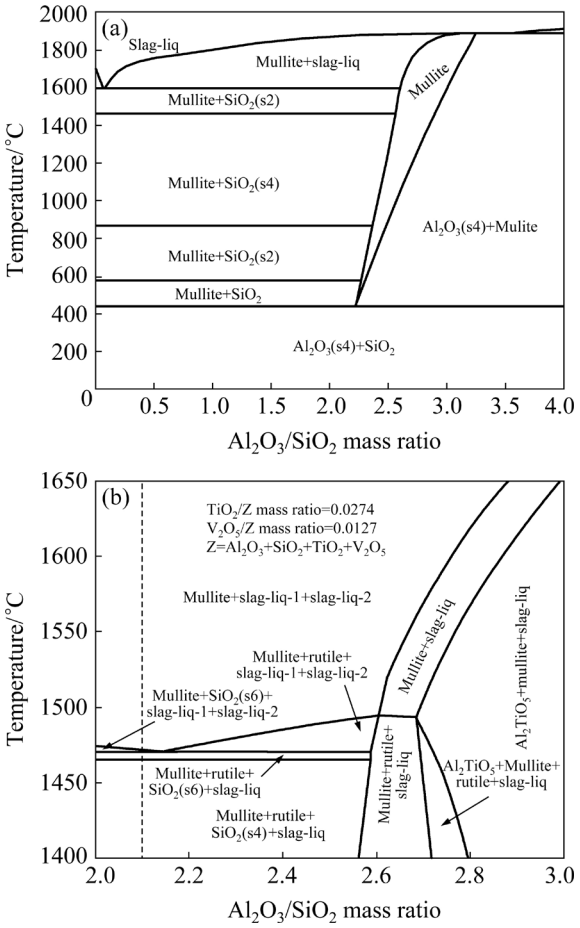

Fig. 2 Phase diagrams of different oxides calculated by FactSage 8.1 under different conditions: (a) Al_2O_3−SiO_2; (b) Al_2O_3−SiO_2−TiO_2−V_2O_5

In this work, the raw material contains a certain amount of V_2O_5 and TiO_2 in addition to Al_2O_3 and SiO_2. According to the mass ratio of V, Ti, Al and Si, the phase diagram of Al_2O_3 and SiO_2 with a certain content of TiO_2 and V_2O_5 is calculated by FactSage 8.1. The results are shown in Fig. 2(b). According to the difference of phases, there are nine regions in Fig. 2(b) when the mass ratio of Al_2O_3 to SiO_2 increases from 2 to 3 and temperature increases from 1400 to 1650 °C. The original mass ratio of Al_2O_3 to SiO_2 in the leaching residue is 2.8. According to Fig. 2(b), Al_2TiO_5, mullite and slag-liq are obtained. However, mullite and liquid slag without Al_2TiO_5 can also be

obtained by changing the mass ratio of Al_2O_3 to SiO_2. When the mass ratio of Al_2O_3 to SiO_2 is 2.1, mullite, slag-liq-1 and slag-liq-2 are obtained above 1500 °C.

Figure 3 shows that the content of each phase changes with temperature from 1400 to 1650 °C at Al_2O_3/SiO_2 mass ratio of 2.1 calculated by FactSage 8.1. In Fig. 3(a) the content of mullite decreases from 90.28 wt.% to 77.98 wt.% and the content of slag-liq-1 increases from 2.92 wt.% to 20.00 wt.% in the temperature range from 1400 to 1650 °C. When the temperature exceeds 1500 °C, the TiO_2 and SiO_2 phases disappear. Figures 3(b) and (c) indicate the compositions of slag-liq-1 phase and slag-liq-2 phase, respectively. Temperature has a great influence on the composition of slag-liq-1 phase. The main compositions of slag-liq-1 phase are Al_2O_3, TiO_2 and V_2O_5 at 1400 and 1450 °C. However, the main compositions of slag-liq-1 phase are Al_2O_3, TiO_2, and SiO_2 above 1500 °C. The slag-liq-2 phase does not appear below 1450 °C. The main compositions of slag-liq-2 phase are Al_2O_3, TiO_2 and V_2O_5 above 1500 °C. In order to synthesize mullite from leaching residue, the temperature and Al_2O_3/SiO_2 mass ratio should be strictly controlled.

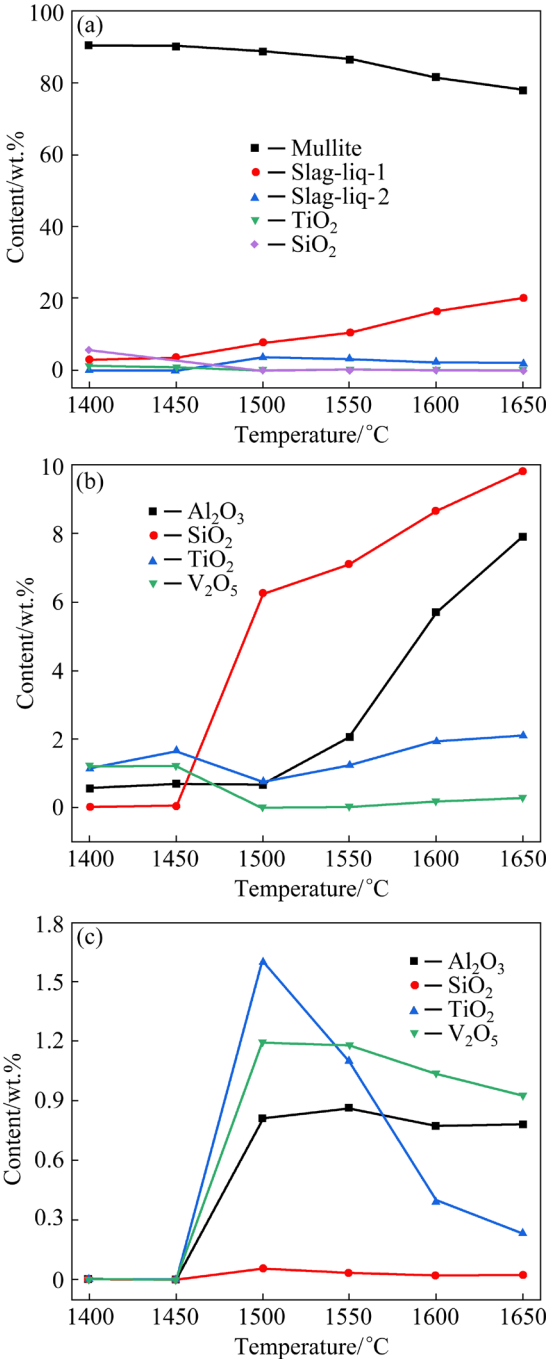

Fig. 3 Content of each phase vs temperature (a), and contents of slag-liq-1 (b) and slag-liq-2 (c) vs temperature at Al_2O_3/SiO_2 mass ratio of 2.1

3.1.2 Effect of Al_2O_3/SiO_2 mass ratio

In order to explore the effect of different proportions of Al_2O_3 and SiO_2, the mass ratios of Al_2O_3 to SiO_2 were adjusted to 2.8, 2.55 and 2.1, respectively, by adding different amounts of SiO_2 into the leaching residue. The samples were roasted at 1600 °C for 5 h. The results are shown in Fig. 4. From Fig. 4(a), it can be seen that when the mass ratios of Al_2O_3 to SiO_2 were 2.8 and 2.55,

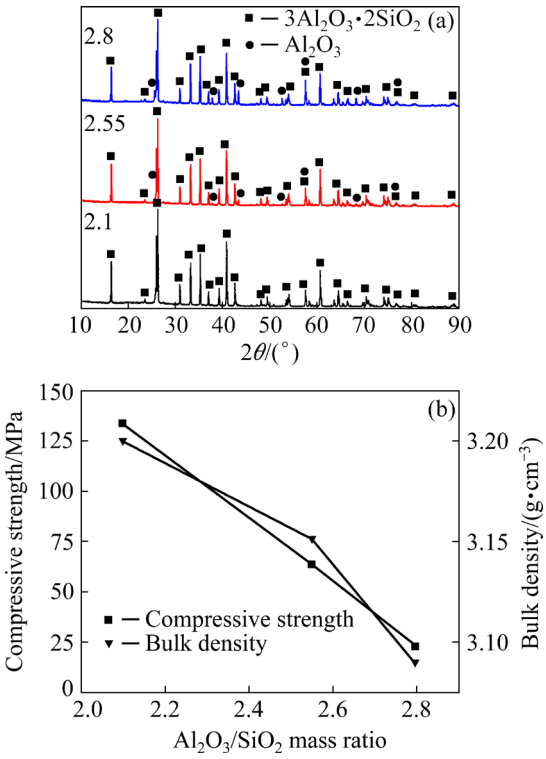

Fig. 4 XRD patterns of mullite synthesized at different Al_2O_3/SiO_2 mass ratios and 1600 °C (a) and effect of Al_2O_3/SiO_2 mass ratio on compressive strength and bulk density (b)

respectively, the main phases in the product were mullite and Al_2O_3. The diffraction peak of Al_2O_3 decreased continuously with the decrease of mass ratio of the Al_2O_3 to SiO_2. When the mass ratio of Al_2O_3 to SiO_2 was adjusted to 2.1, it could be seen that there was no peak of Al_2O_3, and only mullite phase was synthesized. According to the Al_2O_3−SiO_2 binary phase diagram in Fig. 2(a), the synthesized compounds at Al_2O_3/SiO_2 mass ratio of 2.1 were corresponding to the mullite and slag-liq. There were not only Al_2O_3 and SiO_2, but also some TiO_2 and V_2O_5 in the leaching residue. TiO_2 and V_2O_5 could be doped into the mullite. Meanwhile, according to the Fig. 2(b), the mullite and slag-liq were obtained at Al_2O_3/SiO_2 mass ratio of 2.1. In the Factsage 8.1, there was no such database in which elements such as V, Ti and Cr were doped into the mullite phase. However, elements such as V, Ti, and Cr could be doped into the mullite lattice in the roasting process [23,24]. It was reported that Ti^{4+} and V^{5+} replaced Al^{3+} on the octahedra coordination of mullite, which resulted in excessive Al_2O_3 in the leaching residue [25,26]. According to the binary phase diagram of Al_2O_3 and SiO_2, a pure mullite phase could be formed at Al_2O_3/SiO_2 mass ratio of 2.8. However, according to our experimental results, the addition of SiO_2 in the leaching residue could synthesize a pure phase of mullite, which also proved that V and Ti replaced Al in mullite. It can be seen from Fig. 4(b) that the bulk density and compressive strength of the product increased continuously with the decrease of the Al_2O_3/SiO_2 mass ratio. When the Al_2O_3/SiO_2 mass ratio was 2.1, the bulk density (3.20 g/cm^3) and compressive strength (133.345 MPa) of the product reached the maximum. When the phase was not pure, the product contained mullite and Al_2O_3. Meanwhile, the thermal expansion coefficient of Al_2O_3 was different from that of mullite, resulting in uneven shrinkage and residual stress during cooling, which made it difficult to densify. The content of mullite in the product increased continuously with the decrease of Al_2O_3/SiO_2 mass ratio. When the mullite was pure phase, the elemental distribution of product was more uniform. Meanwhile, the residual stress disappeared in the cooling process, and the product was more compact. The compressive strength was improved. Therefore, the optimal Al_2O_3/SiO_2 mass ratio was 2.1.

Figure 5 shows the SEM images of samples with different mass ratios of Al_2O_3 to SiO_2. As shown in Figs. 5(a_1, a_2), the leaching residue without adding SiO_2 formed multi-pores morphology on its surface. There were many large-sized holes and the holes were obviously connected. The average size of pore was around 50.5 μm and the grain size was small. When the Al_2O_3/SiO_2 mass ratio was 2.1, the pore size decreased to 35.4 μm in Figs. 5(c_1, c_2).

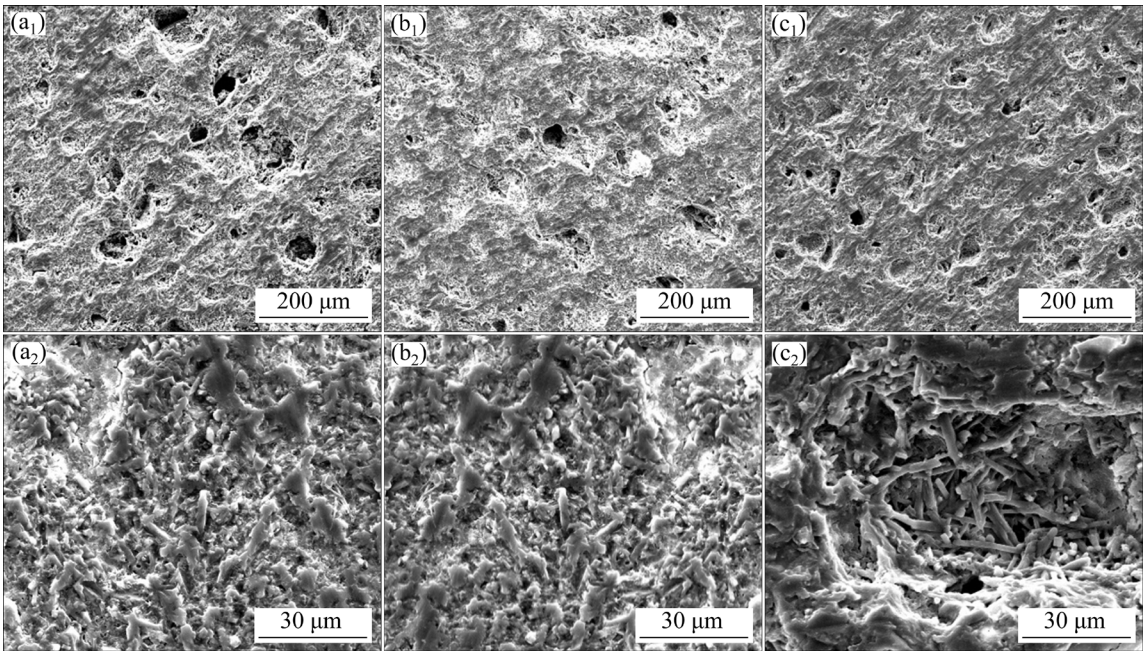

Fig. 5 SEM images of mullite synthesized at different Al_2O_3/SiO_2 mass ratios and 1600 °C for 5 h: (a_1, a_2) 2.8; (b_1, b_2) 2.55; (c_1, c_2) 2.1

This showed that the synthesis of pure mullite could effectively improve the density of the samples. Figures 5(a_2, b_2, c_2) indicated that the mullite containing Al_2O_3 phase almost presented the sintered morphology, which was completely inconsistent with the typical grain morphology of mullite. The grain morphology of mullite was caused by the anisotropic crystallization behavior of mullite.

3.1.3 Effects of temperature and time on mullite

When the Al_2O_3/SiO_2 mass ratio was adjusted to 2.1, the phases of the products obtained at different reaction temperatures and time were shown in Figs. 6(a, c), respectively. The synthesized products at 1400 and 1500 °C were mainly mullite and Al_2O_3, and the diffraction peak of Al_2O_3 decreased with the increase of temperature. When the temperature increased to 1600 °C, pure mullite was synthesized, and the diffraction peak of Al_2O_3 was not detected in the phase. Since the reaction type was mainly solid−solid reaction, the diffusion ratio of Si to Al atoms was slow, and the contact and reaction needed to be completed at high temperature. It could be seen from Fig. 6(a) that the diffraction peak of the product obtained at 1600 °C was narrower and sharper than that at 1400 and 1500 °C, which showed that the crystallinity of product was better. When the reaction temperature was 1600 °C, the sintering driving force increased. Meanwhile, the residual voids were reduced, and the rapid growth of mullite grains was promoted. It could be seen from Fig. 6(b) that the bulk density and compressive strength of the products increased with the increase of temperature. When the temperature reached 1600 °C, the bulk density and compressive strength of the product reached the maximum. High temperature is conducive to the progress of solid-phase reactions. Meanwhile, the liquid phase also gradually increased with the increase of temperature, which reduced the residual voids in the product, and promoted the rapid growth of mullite grains and the densification of the product. The pure mullite made the composition of the product more uniform and reduced the possibility of cracks. The product synthesized at 1600 °C was pure mullite, and the bulk density and compressive strength reached the maximum value. Although the temperature was relatively high, it could be seen that the product synthesized at low temperature with water leaching residue as raw material was

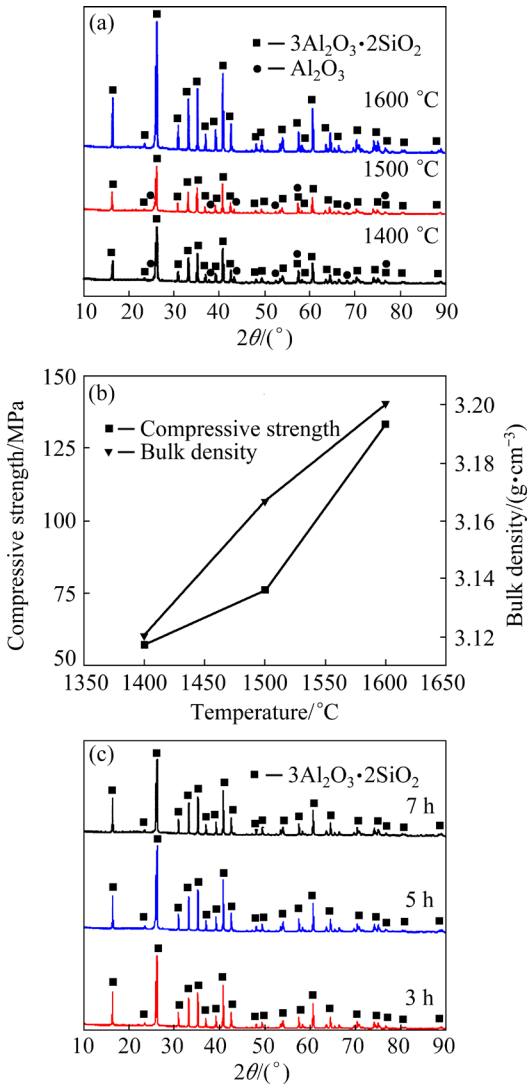

Fig. 6 XRD patterns of mullite synthesized at different temperatures and Al_2O_3/SiO_2 mass ratio of 2.1 (a), effect of temperature on compressive strength and bulk density (b), and XRD patterns of mullite synthesized at different time, Al_2O_3/SiO_2 mass ratio of 2.1 and 1600 °C (c)

impure and had poor mechanical properties. In order to ensure the purity of the product and improve the performance of the product, 1600 °C was selected as the reaction temperature. The effect of time on synthesized mullite was shown in Fig. 6(c). Pure mullite could be synthesized when the reaction time was 3 h. However, the diffraction peak of mullite at 5 h was stronger than that at 3 h, which indicated that the crystallinity of mullite increased. However, the increase of diffraction peak of mullite was not obvious with time from 5 to 7 h.

Figure 7 shows the SEM images of mullite at different time. It was found that the pore size decreased from 41.29 to 35.4 μm with the incrase of

reaction time from 3 to 5 h. When the reaction time increased from 5 to 7 h, and the pore size decreased from 35.4 to 34.5 μm. Meanwhile, it was found that the grain size was small and the bonding phenomenon was serious at 3 h. The grain was coarse and the bonding phenomenon was less at 5 h. As the reaction time increased from 5 to 7 h, the pore size and morphology had little difference. Therefore, the optimal reaction time was 5 h.

3.1.4 Mechanical properties

The influence of structural factors such as pores, main crystalline phase and glass pahse in mullite on the mechanical properties of the material works by inhibiting or inducing microcracks [27]. Table 2 shows the comparison of compressive strength and bulk denstiy of mullite in this work and Refs. [28−34]. It is found that the pure phase mullite synthesized in this work has better compressive strength and higher bulk density than the mullite in the literature. This is because trace amount of elements Ti and V in the leaching residue form a partial liquid phase at high temperature and enter the cracks to promote the densification of mullite. Meanwhile, according to the above analysis, the mullite obtained in this work was pure phase and the surface was dense. In view of the fact that the pressure at which the sample was pressed was only 20 MPa, it could be considered that the raw material has good binding properties under high temperature conditions.

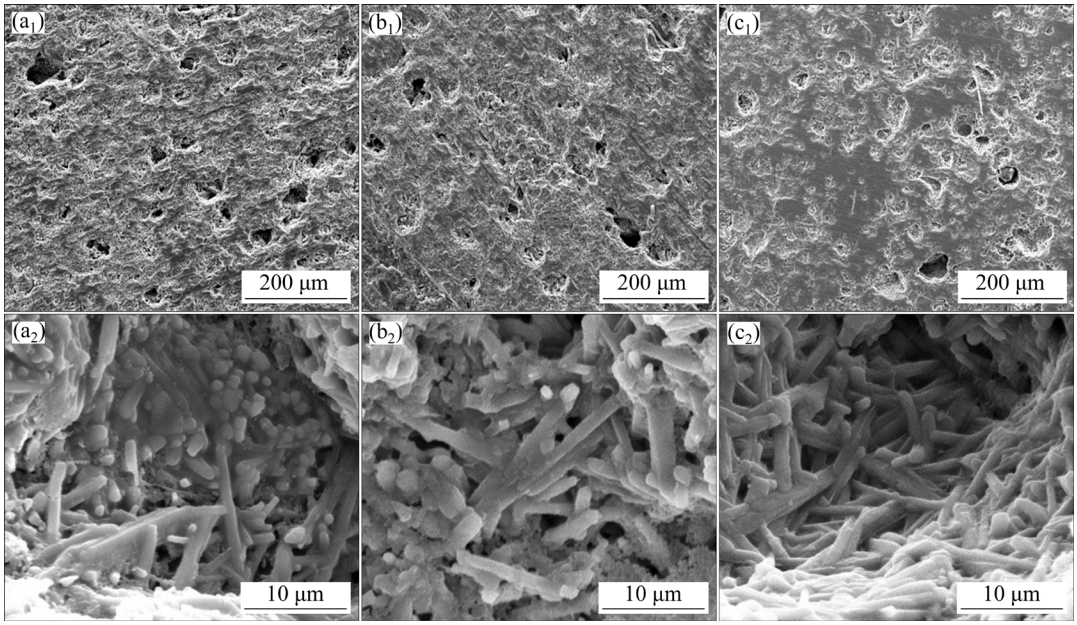

Fig. 7 SEM images of mullite synthesized at 1600 °C and different time: (a_1, a_2) 3 h; (b_1, b_2) 5 h; (c_1, c_2) 7 h

Table 2 Comparison of compressive strength and bulk density of mullite synthesized in this work and reported in Refs. [28−34]

Material	Temperature/°C	Time/h	Compressive strength/MPa	Bulk density/(g·cm^{-3})	Source
Vanadium slag	1600	5	133.35	3.20	Present work
Commercial grade mullite powder	1500	2	108		[28]
Commercially fused mullite powder	1500	5	11.68	0.7	[29]
Analytical grade Al_2O_3 and SiO_2	1700	6	178	2.77	[30]
Ammonium hexafluoroaluminate and kaolinite	1550	2		3.16	[31]
High-aluminum fly ash	1600	2		2.85	[32]
High-aluminum fly ash	1600	2	169	2.78	[33]
High-iron bauxite	1700	2	105		[34]

3.2 Toxicity identification of synthetic mullite

3.2.1 Stabilization effect of pure mullite on impurity ions of Cr, V, and Ti

Table 3 shows that the synthesized pure phase mullite also contains a small amount of impurity oxides (V, Cr, Ti, Mn and Fe). Howerver, Cl was not detected. Cl^- in the leaching residue was volatilized during the high-temperature reaction. Thus, Cl^- in the mullite was removed. As we all know, high-valent V and Cr are harmful to the environment. Thus, it is necessary to determine the valence and distribution of impurity oxides in mullite.

From the EDS spectra in Fig. 8, the elements Cr, Mn, V, and Ti are uniformly distributed in the mullite phase, which are consistent with the distribution of elements Al and Si, indicating that the metal ions (V, Ti, Cr, Mn, and Fe) entered the mullite lattice to form a solid solution. Valences of V and Ti in mullite were analyzed by XPS. According to Fig. 9, V and Ti in mullite existed in the form of V^{5+} and Ti^{4+} phases, respectively. The binding energy of 524.38 eV for V $2p_{2/3}$ and that of 516.88 eV for V $2p_{1/2}$ are attributed to the V^{5+}. Meanwhile, the binding energy of 464.5 eV for Ti $2p_{2/3}$ and that of 458.8 eV for Ti $2p_{1/2}$ are attributed to the Ti^{4+}. The ionic radii of Ti^{4+} (60.5 pm) and V^{5+}(59 pm) were larger than that of Al^{3+}(53.5 pm), the formation mechanism of the solid solution was the uniform and equivalent replacement of Al distributed in the octahedron of the mullite lattice by elements V and Ti. Thus, V^{5+} and Ti^{4+} were easy to form octahedral coordination of solid solution. It could be proved that the trace impurity elements in mullite were stabilized in the mullite phase.

Figure 10 shows the TEM images of pure mullite synthesized by doping trace elements. The crystal structure of mullite was roughly columnar, and the typical orthogonal structure could be seen in the selected area electron diffraction (SAED) pattern. The growth direction of mullite was (210) orientation. By the comparison of SAED, the single

Table 3 Composition of synthetic pure mullite (wt.%)

Al_2O_3	SiO_2	TiO_2	V_2O_5	Fe_2O_3	MnO	Cr_2O_3
63.6	31.3	2.43	1.14	0.255	0.0214	0.163

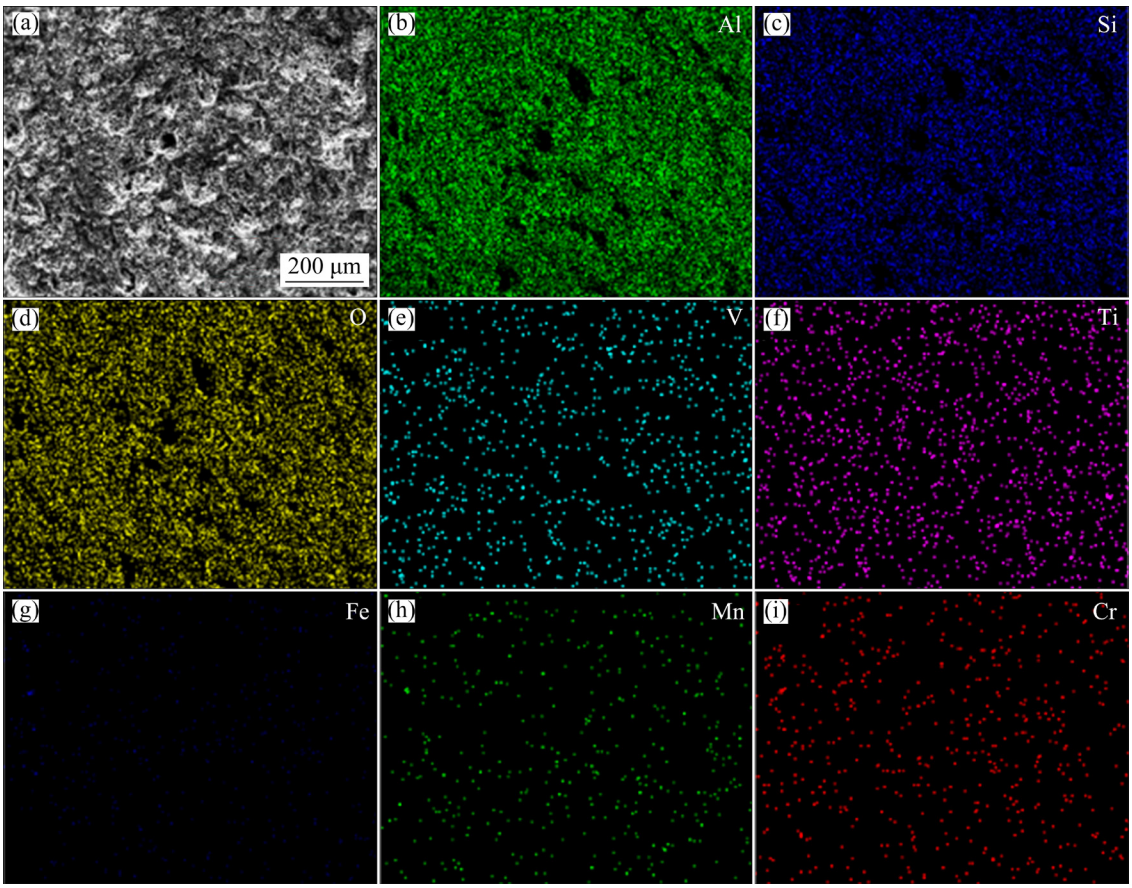

Fig. 8 Element distribution maps obtained by EDS scanning of pure mullite

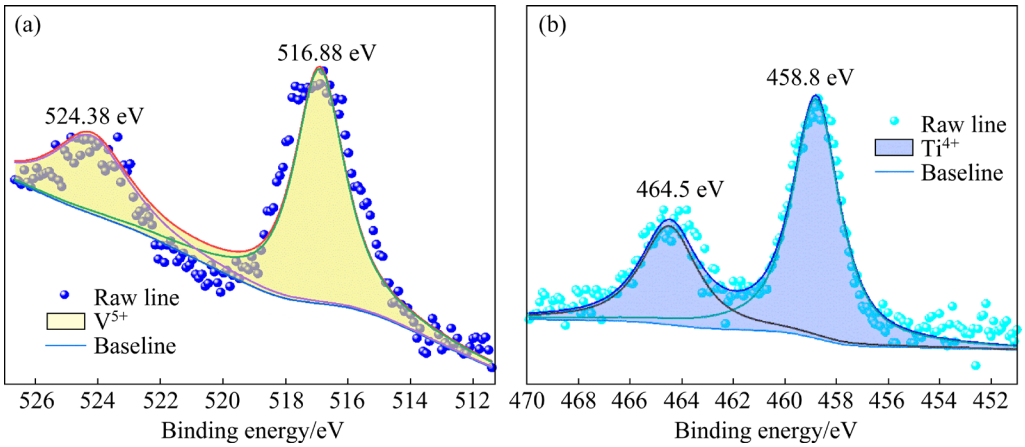

Fig. 9 XPS valence analysis results of V (a) and Ti (b)

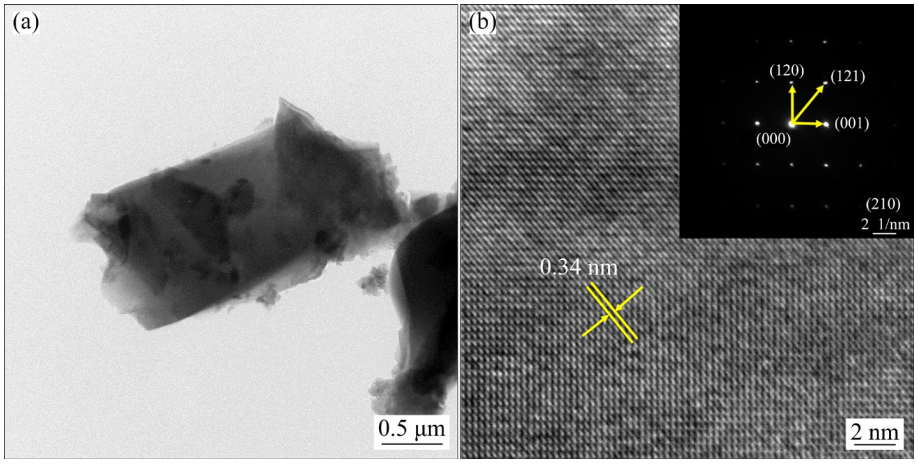

Fig. 10 TEM image (a), and TEM lattice image and SAED pattern (b) of pure mullite synthesized at Al_2O_3/SiO_2 mass ratio of 2.1 and 1600 °C for 5 h

crystal mullite with Al/Si molar ratio of 3/1 was synthesized. The reason why the crystal structure of mullite is not regularly columnar is due to the doping of metal elements (Mn, Fe, Cr, Ti, and V) in leaching residue. Because the ionic radius of V^{5+} and Ti^{4+} is higher than that of Al^{3+}, the morphology is slightly deformed during the doping process.

According to the high-resolution transmission electron microscopy (HRTEM) image, the crystal plane spacing of the sample was 0.34 nm, corresponding to (210) crystal plane. However, the crystal plane spacing of the sample synthesized with pure substance was about 0.531 nm [35]. The change of crystal plane spacing indicated that trace elements were doped into mullite phase. The smaller the crystal spacing is, the greater the adjacent crystal face attracts. The crystal will grow rapidly in this direction. However, the rapidly growing crystals will form more nuclei. Thus, many irregular grains will be formed. This is the growth behavior of mullite crystals doped with trace elements.

3.2.2 Identification of leaching toxicity of synthetic mullite

According to the above analysis, the hazardous element V in the pure mullite exsited in the form the V^{5+}. If the hazardous elements V, Cr, and Mn cannot be stabilized to enter the mullite phase, they will harm to the environment. Thus, in order to determine the toxicity of synthesized pure mullite, the toxicity of mullite was determined by ICP-AES using USEPA 1311 TCLP standard. The results are shown in Table 4 and Fig. 11. All the elements concentrations contained in the leaching residue were far lower than the TCLP standard, and the main metal elements such as V, Cr, Fe, Mn and Ti remaining in the leaching residue were stabilized in mullite.

The calculation formula of leaching rate is shown as follows:

Table 4 Toxicity test results of pure mullite measured according to TCLP standard (mg/L)

Item	Cr	Mn	Fe	Cu	As	Cd
TCLP standard	5			15	5	1
Leaching residue	0.103	0.450	3.267	0.242	0.168	0.019
Item	Ba	Pb	Zn	Ag	V	Ti
TCLP standard	100	5	100	5		
Leaching residue	0.095	0.260	0.45	−	4.759	0.264

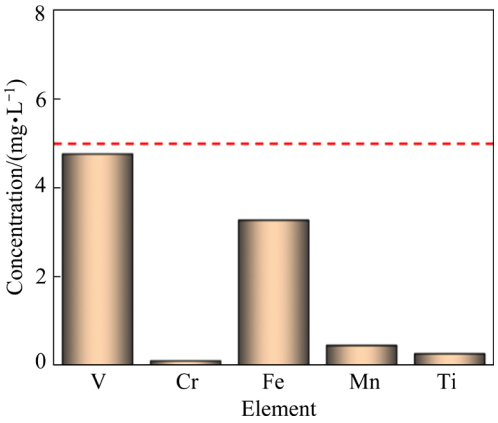

Fig. 11 Toxicity test results of pure mullite

$$\mu_{(V,Ti)}=\frac{C_{(V,Ti)}V}{m_{(V,Ti)}}\times 100\% \quad (1)$$

where $\mu_{(V,Ti)}$ is the leaching rate of V and Ti; $C_{(V,Ti)}$ is the concentration of V and Ti in the leachate (g/L); V is the volume of leachate (L); $m_{(V,Ti)}$ is the mass of V and Ti in the product after vanadium slag pretreatment (g).

According to Eq. (1) it is obtained that the leaching rate of V is 1.3% and that of Ti is only 0.03%.

In order to ensure the generality of the results, the toxicity leaching of mullite was determined by the GB 5085.3—2007 standard. The results are shown in Table 5. According to the standard, pure mullite synthesized from vanadium slag is a non-toxic product, the content of all elements is far below the national standard. The main metal elements such as V, Cr, Fe, Mn and Ti remained in the leaching residue were stabilized in mullite. After calculation, it was found that the leaching rates of these elements are less than 1%. The leaching rate of V is less than 0.05%, the leaching rate of Ti is only 0.002%, and the leaching rate of Cr is too low to be detected.

Table 5 Toxicity test results of pure mullite measured according to GB 5085.3—2007 standard (mg/L)

Item	V	Ti	Cr	Mn	Fe	Be	Cu
GB standard			15			0.02	100
Leaching residue	0.374	0.036	−	0.343	0.928	−	0.232
Item	As	Cd	Ni	Ba	Pb	Zn	Ag
GB standard	5	1	5	100	5	100	5
Leaching residue	0.075	−	0.039	0.03	−	0.45	0.017

This result not only confirms that the residual hazardous elements V and Cr are stabilized in the mullite product, but also guarantees the environmental safety of the pure mullite.

In the process of comprehensive utilization of vanadium slag, the molten salt chlorination of vanadium slag with $AlCl_3$ under optimal conditions can increase the chlorination rate of V, Cr, Fe and Mn in vanadium slag to 76.5%, 81.9%, 90.3% and 97.3%, respectively. The volatilization rate of Ti increases to 79.9% [11]. The pure-phase mullite synthesized from the water leaching residue after removing all chlorinated products was found to be able to effectively stabilize the remaining hazardous elements according to the GB 5085.3 — 2007 standard. That is to say, the leaching residue containing hazardous elements V, Cr and Mn can be converted from hazardous solid waste into safe and nontoxic pure mullite produt by this one-step solid state reaction.

4 Conclusions

(1) Pure mullite was synthesized by high temperature roasting of leaching residue, and high value-added utilization of leaching residue was realized. Mullite with high compressive strength of 133.35 MPa and bulk density of 3.20 g/cm^3 was synthesized by using leaching residue as raw material, adding appropriate SiO_2 (the Al_2O_3/SiO_2 mass ratio was 2.1) and roasting at 1600 °C for 5 h.

(2) Elements such as V, Cr, Fe, Mn and Ti were stabilized in the mullite phase in the form of solid solution, in which V and Ti exist in the form of V^{5+} and Ti^{4+} phases, respectively.

(3) According to TCLP standard and GB 5085.3—2007 standard, the toxicity of mullite was identified. The mullite was a nontoxic product. This novel method has certain reference siginificance for the treatment of waste resiues containing hazardous elements.

Acknowledgments

The authors are grateful for the financial supports from the National Natural Science Foundation of China (Nos. 51922003, 51904286, 51774027, 51734002).

References

[1] LIU Shi-yuan, HE Xiao-bo, WANG Ya-dun, WANG Li-jun. Cleaner and effective extraction and separation of iron from vanadium slag by carbothermic reduction-chlorination-molten salt electrolysis [J]. Journal of Cleaner Production, 2021, 284: 124674.

[2] XIANG Jun-yi, WANG Xin, PEI Gui-shang, HUANG Qing-yun, LÜ Xue-wei. Recovery of vanadium from vanadium slag by composite roasting with CaO/MgO and leaching [J]. Transactions of Nonferrous Metals Society of China, 2020, 30(11): 3114−3123.

[3] LIU Shi-yuan, YE Lin, WANG Li-jun, CHOU Kuo-chih. Selective oxidation of vanadium from vanadium slag by CO_2 during $CaCO_3$ roasting treatment [J]. Separation and Purification Technology, 2023, 312: 123407.

[4] WANG Xue-wen, YANG Ming-e, MENG Yu-qi, GAO Da-xing, WANG Ming-yu, FU Zi-bi. Cyclic metallurgical process for extracting V and Cr from vanadium slag: Part I. Separation and recovery of V from chromium-containing vanadate solution [J]. Transactions of Nonferrous Metals Society of China, 2021, 31(3): 807−816.

[5] HAN Ji-qing, ZHANG Jing, ZHANG Jia-hao, CHEN Xiao, ZHANG Li, TU Gan-feng. Recovery of Fe, V, and Ti in modified Ti-bearing blast furnace slag [J]. Transactions of Nonferrous Metals Society of China, 2022, 32(1): 333−344.

[6] LIU Shi-yuan, WANG Li-jun, CHOU Kuo-chih. Innovative method for minimization of waste containing Fe, Mn and Ti during comprehensive utilization of vanadium slag [J]. Waste Management, 2021, 127: 179−188.

[7] LIU Yi, LI Lan-jie, WANG Chun-mei, DENG Wen-xiang, ZHOU Bing-jing. Resource utilization technology of vanadium extraction tailings [J]. Hebei Metallurgy, 2020(6): 79−82. (in Chinese)

[8] LI Peng-wei, LUO Shao-hua, WANG Jia-chen, WANG Yu-he, WANG Qing, ZHANG Ya-hui, LIU Xin, GAO De-sheng, LV Fang, MU Wen-ning, LIANG Jin-sheng, DUAN Xin-hui. Extraction and separation of Fe and Ti from extracted vanadium residue by enhanced ammonium sulfate leaching and synthesis of $LiFePO_4$/C for lithium-ion batteries [J]. Separation and Purification Technology, 2022, 282: 120065.

[9] ZHANG Ju-hua, ZHANG Wei, ZHANG Li, GU Song-qing. Mechanism of vanadium slag roasting with calcium oxide [J]. International Journal of Mineral Processing, 2015, 138: 20−29.

[10] LI Peng-wei, LUO Shao-hua, FENG Jian, LV Fang, YAN Sheng-xue, WANG Qing, ZHANG Ya-hui, MU Wen-ning, LIU Xin, LEI Xue-fei, TENG Fei, LI Xian, CHANG Long-jiang, LIANG Jin-sheng, DUAN Xin-hui. Study on the high-efficiency separation of Fe in extracted vanadium residue by sulfuric acid roasting and the solidification behavior of V and Cr [J]. Separation and Purification Technology, 2021, 269: 118687.

[11] LIU Shi-yuan, WANG Li-jun, CHOU Kuo-chih. A novel process for simultaneous extraction of iron, vanadium, manganese, chromium, and titanium from vanadium slag by molten salt electrolysis [J]. Industrial & Engineering Chemistry Research, 2016, 55(50): 12962−12969.

[12] RAMEZANI A, EMAMI S M, NEMAT S. Reuse of spent FCC catalyst, waste serpentine and kiln rollers waste for synthesis of cordierite and cordierite−mullite ceramics [J]. Journal of Hazardous Materials, 2017, 338: 177−185.

[13] WANG Wei-chao, MCCOOL G, KAPUR N, YUAN Guang, SHAN Bin, NGUYEN M, GRAHAM U M, DAVIS B H, JACOBS G, CHO K, HAO Xiang-long. Mixed-phase oxide catalyst based on Mn-mullite (Sm,Gd)Mn_2O_5 for NO oxidation in diesel exhaust [J]. Science, 2012, 337: 832−835.

[14] ZHENG Yong-ping, THAMPY S, ASHBURN N, DILLON S, WANG Lu-hua, JANGJOU Y, TAN Kui, KONG Fan-tai, NIE Yi-fan, KIM M J, EPLING W S, CHABAL Y J, HUS J P, CHO K Y. Stable and active oxidation catalysis by cooperative lattice oxygen redox on $SmMn_2O_5$ mullite surface [J]. Journal of the American Chemical Society, 2019, 141(27): 10722−10728.

[15] LI Na, ZHANG Xiao-yan, QU Ya-nan, XU Jie, MA Ning, GAN Ke, HUO Wen-long, YANG Jin-long. A simple and efficient way to prepare porous mullite matrix ceramics via directly sintering SiO_2−Al_2O_3 microspheres [J]. Journal of the European Ceramic Society, 2016, 36: 2807−2812.

[16] LIU Rui-li, DONG Xue, XIE Shuang-tian, JIA Tao, XUE Yun-jia, LIU Jia-chen, JING Wei, GUO An-ran. Ultralight, thermal insulating, and high-temperature-resistant mullite-based nanofibrous aerogels [J]. Chemical Engineering Journal, 2019, 360: 464−472.

[17] WAN Xiang, WANG Li, GAO Shan, LANG Xiu-yao, WANG Lin-xia, ZHANG Tong, DONG An-qi, WANG Wei-chao. Low-temperature removal of aromatics pollutants via surface labile oxygen over Mn-based mullite catalyst $SmMn_2O_5$ [J]. Chemical Engineering Journal, 2021, 410: 128305.

[18] SCHNEIDER H, FISCHER R X, SCHREUER J. Mullite: Crystal structure and related properties [J]. Journal of the American Ceramic Society, 2015, 98: 2948−2967.

[19] CHEN Ming-liang, ZHU Li, DONG Ying-chao, LI Ling-ling, LIU Jing. Waste-to-resource strategy to fabricate highly porous whisker-structured mullite ceramic membrane for simulated oil-in-water emulsion wastewater treatment [J]. ACS Sustainable Chemistry & Engineering, 2016, 4(4): 2098−2106.

[20] LI Guang-hui, BU Qun-zhen, SUN Hu, SHI Da-peng, LUO Jun, RAO Ming-jun, PENG Zhi-wei, JIANG Tao. Cost-effective and sustainable preparation of porous mullite-based

ceramics combining MoO_3 recovery from industrial calcine [J]. ACS Sustainable Chemistry & Engineering, 2020, 8(19): 7290−7299.

[21] SCHNEIDER H, RAGER H. Occurrence of Ti^{3+} and Fe^{2+} in mullite [J]. Journal of the American Ceramic Society, 1984, 67: c248−c250.

[22] ZHANG Wei, MA Qing-song, DAI Ke-wei, MAO Wei-guo. Preparation of three-dimensional braided carbon fiber reinforced mullite composites from a sol with high solid content [J]. Transactions of Nonferrous Metals Society of China, 2018, 28(11): 2248−2254.

[23] KLOCHKOVA I V, DUDKIN B N, SHVEIKIN G P, GOLDIN B A, NAZAROVA L Y. The effect of sesquioxides of 3d-transition elements on the strength of synthetic mullite and mullite-based materials [J]. Refractories and Industrial Ceramics, 2001, 42(9): 351−354.

[24] SARIN P, YOON W, HAGGERTY R P, CHIRITESCU C, BHORKAR N C, KRIVEN W M. Effect of transition-metal-ion doping on high temperature thermal expansion of 3: 2 mullite—An in situ, high temperature, synchrotron diffraction study [J]. Journal of the European Ceramic Society, 2008, 28: 353−365.

[25] ROY J, BANDYOPADHYAY N, DAS S, MAITRA S. Role of V_2O_5 on the formation of chemical mullite from aluminosilicate precursor [J]. Ceramics International, 2010, 36: 1603−1608.

[26] SUHASINEE B P, BHATTACHARYYA S. Sintering and microstructural study of mullite prepared from kaolinite and reactive alumina: effect of MgO and TiO_2 [J]. International Journal of Applied Ceramic Technology, 2021, 18(1): 81−90.

[27] MEN Dan-ju. Processing and characterization of multiphase ceramic composites [D]. Irvine: University of California, 2012.

[28] BODHAK S, BOSE S, BANDYOPADHYAY A. Densification study and mechanical properties of microwave-sintered mullite and mullite–zirconia composites [J]. Journal of the American Ceramic Society, 2011, 94(1): 32−41.

[29] YANG Feng-kun, LI Cui-wei, LIN Ya-mei, WANG Chang-an. Effects of sintering temperature on properties of porous mullite/corundum ceramics [J]. Materials Letters, 2012, 73: 36−39.

[30] YE Hang, LI Yong, SUN Jia-lin, SUN Yang, WU Xiao-fang, YAN Ming-wei. Novel iron-rich mullite solid solution synthesis using fused-silica and α-Al_2O_3 powders [J]. Ceramics International, 2019, 45(4): 4680−4684.

[31] XU Lin-feng. Preparation of mullite porous ceramic with high porosity through a solid-phase sintering process [D]. Guangzhou: South China University of Technology, 2015. (in Chinese)

[32] ZHANG Jian-bo, LI Shao-peng, LI Hui-quan, WU Qi-sheng, XI Xin-guo, LI Zhan-bing. Preparation of Al−Si composite from high-alumina coal fly ash by mechanical–chemical synergistic activation [J]. Ceramics International, 2017, 43(8): 6532−6541.

[33] LIN Bin, LI Shao-peng, HOU Xin-juan, LI Hui-quan. Preparation of high performance mullite ceramics from high-aluminum fly ash by an effective method [J]. Journal of Alloys and Compounds, 2015, 623: 359−361.

[34] ZHAO Fei, GE Tie-zhu, GAO Jin-xing, CHEN Liu-gang, LIU Xin-hong. Transient liquid phase diffusion process for porous mullite ceramics with excellent mechanical properties [J]. Ceramics International, 2018, 44(16): 19123−19130.

[35] LI Wei, ZHANG Jie, LI Xiang-cheng, GONG Wei, CHEN Ping-an, ZHU Bo-quan. Synthesis and electromagnetic properties of one-dimensional La^{3+}-doped mullite based on first-principles simulation [J]. Ceramics International, 2019, 45(14): 17325−17335.

高温反应合成莫来石实现钒渣氯化残渣的无毒高效利用

刘仕元[1]，薛未华[1]，王丽君[1]，周国治[2]

1. 北京科技大学 钢铁共性技术协同创新中心，北京 100083；
2. 北京科技大学 钢铁冶金新技术国家重点实验室，北京 100083

摘　要：采用氯化法从钒渣中提取有价元素(Ti、Cr、Fe、Mn 和 V)后得到的浸出渣主要成分为 Al_2O_3 和 SiO_2，还含有少量有害元素 Cr 和 V。为了减少 Cr 和 V 对环境的污染，提出一种浸出渣无毒和有效利用的新方法。以浸出渣为原料，加入适量 SiO_2，在 1600 ℃下固相烧结 5 h，合成抗压强度为 133.345 MPa、密度为 3.20 g/cm^3 的纯莫来石。浸出渣中的微量元素 Ti 和有害元素 V 和 Cr 在高温反应过程中进入莫来石晶格形成固溶体，稳定在莫来石相中。合成的样品采用毒性特性浸出程序(TCLP)和 GB5085.3—2007 进行检测。结果表明，莫来石符合毒性浸出标准，是一种安全无毒产品。

关键词：浸出残渣；钒渣；综合利用；高毒性六价铬；莫来石；毒性特性浸出程序

(Edited by Wei-ping CHEN)